

Dynamic sparse graphs with overlapping communities

Antreas Laos

Department of Computer Science, University of Cyprus
and

Xenia Misouridou*

Department of Mathematics and Statistics, University of Cyprus

Department of Mathematics, Imperial College London
and

Francesca Panero†

Department of Methods and Models for Economics, Territory and Finance,
Sapienza University of Rome

Department of Statistics, London School of Economics and Political Science

Abstract

Dynamic community detection in networks addresses the challenge of tracking how groups of interconnected nodes evolve, merge, and dissolve within time-evolving networks. Here, we propose a novel statistical framework for sparse networks with power-law degree distribution and dynamic overlapping community structure. Using a Bayesian Nonparametric framework, we build on the idea to represent the graph as an exchangeable point process on the plane. We base the model construction on vectors of completely random measures and a latent Markov process for the time-evolving node affiliations. This construction provides a flexible and interpretable approach to model dynamic communities, naturally generalizing existing overlapping block models to the sparse and scale-free regimes. We provide the asymptotic properties of the model concerning sparsity and power-law behavior and propose inference through an approximate procedure which we validate empirically. We show how the model can uncover interpretable community trajectories in a real-world network.

Keywords: Temporal Network Modelling, Dynamic Mixed Memberships, Vectors of Completely Random Measures, Markov Process, Sparsity, Degree Heterogeneity

* *XM has received funding from the European Union’s Horizon Europe research and innovation programme under Marie Skłodowska-Curie for the project “DyNeMo”, id 101151781.*

† *FP has received funding from Sapienza University of Rome for the project “Bayesian models for sparse networks and applications” grant number RP1241910EF9AF1F.*

1 Introduction

Networks or graphs are mathematical structures that allow us to represent the relationships between a set of entities. These entities can be people, organizations, and they have various applications across the social sciences, biology, finance, economy and technology. For an overview see for example [Newman \(2010\)](#) or [Kolaczyk \(2009\)](#). A generic network comprises of a set of nodes with edges between them and the degree of a node is the number of edges connected to it. The rate of growth of the number of edges in relation to the number of nodes defines the density (or sparsity) level of a graph. Intuitively, a dense network appears when the number of edges scales quadratically with the number of nodes, while a sparse network arises when this relation is subquadratic.

One of the central tasks in statistical network modeling is to be able to identify latent communities, i.e. groups of nodes that exhibit some sort of similar behavior and usually have comparable connectivity patterns. This is useful as real-world networks (social, biological, technological or others) often have modular structure ([Newman 2006](#), [Fortunato 2010](#)). Community detection helps us uncover groups of nodes that are more densely connected internally than externally, revealing the hidden organization of the system. In social networks, communities may be social groups or interest circles. In information networks, communities identify related topics or content clusters (e.g., news or articles, research topics). In economics, they can highlight groups of markets or firms that interact closely.

While static graph models have been widely applied, many real-world networks are inherently dynamic. The links between the nodes change in time as well as the community structure. For example, in a social network new connections appear or existing ones disappear, and similarly the communities are not static, as friend groups form, evolve, and dissolve over time showing us how social ties strengthen, weaken, or reorganize. In information networks such as citation or news networks, dynamic communities uncover how

topics appear, merge, or fade with time, which can shed light into the evolution of new fields, trends in online media, or shifting patterns of information diffusion. Therefore, in such settings a static analysis that aggregates the graph across time will obscure important features, such as the rate of turnover in membership, or the emergence of new groups. Hence, we need a class of dynamic communities network models that can characterize not only the structure of a network at a given moment, but also its evolutionary mechanisms such as whether communities are stable or transient, whether entities tend to remain in the same group or switch groups, and how global (macro) structural changes propagate through the system. Incorporating temporal dependence and temporal correlation allows for information to be shared across adjacent time points rather than treating each timestep in isolation of the others.

Stochastic block models (SBMs) and their extensions have proven useful in statistics for modeling networks. Following the well celebrated static SBM, dynamic variations were introduced by [Matias & Miele \(2017b\)](#), [Xu & Hero \(2013\)](#), [Xu et al. \(2012\)](#), [Yang et al. \(2011\)](#). Although they have some differences (e.g. in inference) all these perform hard dynamic clustering on a graph. In the static case, [Airoldi et al. \(2008\)](#) proposed the mixed membership SBM. In the dynamic case [Xing et al. \(2010\)](#) proposed a mixed membership model with nodes having ‘roles’ and Logistic-normal role vectors with linear Gaussian state-space evolution. Inference is carried out through a variational Bayes expectation–maximization algorithm. [Fu et al. \(2009\)](#) is a previous and more concise version of [Xing et al. \(2010\)](#), and [Ho et al. \(2011\)](#) also propose a dynamic mixed membership SBM. In similar spirit, other authors proposed dynamic models such as [Ishiguro et al. \(2010\)](#), who give a dynamic infinite relational model, and [Herlau et al. \(2013\)](#) who deal with temporal networks of multiscale structure (vertices belong to a hierarchy of groups and subgroups). This list of papers is non-exhaustive, especially if one considers specific applications, e.g.

see [Martinet et al. \(2020\)](#) who extract dynamic communities based on the explicit notion of time-evolving aggregations of smaller motifs on brain networks. Other network approaches which work on the latent space are [Hoff \(2009\)](#), [Hoff et al. \(2002\)](#), [Sarkar & Moore \(2005\)](#), and [Xu & Zheng \(2009\)](#). Of course, beyond the task of community detection there are more time-varying graph models, such as the model for change point detection by [Wilson et al. \(2019\)](#). Similarly, if one goes beyond the scope of statistical models, current literature of deep learning on graphs exists. This is not within the scope of this paper, but for an overview on Graph Neural Networks see e.g. [Wu et al. \(2022\)](#).

Classically, in a large number of papers, graphs were represented by the adjacency matrix of connections. At the same time, for both theoretical and practical reasons it was convenient to make an assumption of exchangeability. Under the adjacency matrix representation, exchangeability means that the graph's distribution is invariant to permutations of the nodes. However, Bayesian graphs that are represented by an exchangeable random array are necessarily either empty or dense ([Lovász 2013](#), [Orbánz & Roy 2015](#)). This is also a persistent limitation of most existing dynamic SBMs, which is undesirable as many observed networks are sparse ([Newman 2010](#), [Orbánz & Roy 2015](#)). Additionally, many sparse graphs exhibit heavy-tailed and power-law degree distributions, meaning that they have a few highly connected nodes and a large number of nodes with few connections (in particular, a large share has only one connection).

Combining exchangeability and sparsity is non-trivial. A solution was given by [Caron & Fox \(2017\)](#) who proposed an alternative way to model graphs that are distributionally invariant but range from dense to sparse, relying on a point process construction and its corresponding definition of exchangeability ([Kallenberg 1990](#)). A series of papers followed this construction ([Borgs et al. 2018](#), [Veitch & Roy 2015](#), [Todeschini et al. 2020](#), [Naik et al. 2022](#), [Herlau et al. 2014](#), [Ricci et al. 2022](#)), none of which allows for dynamic communities.

Here, we propose a novel Bayesian nonparametric model, for dynamic sparse graphs with overlapping communities (dynSNetOC). Our model admits:

1. dynamic connectivity (with nodes and edges allowed to appear or disappear);
2. dynamic mixed membership community affiliations for each node;
3. sparsity and power-law degree distribution;
4. interpretable parameters and uncertainty quantification.

Sparsity and power-law are achieved using exchangeable random measures. The dynamic community behavior arises from a latent Markov process and, as the community affiliations of the nodes vary, the connectivity also changes. Note that with the first point we also allow for nodes to enter later or exit earlier as opposed to other approaches which require the number of nodes to remain constant (e.g. [Kang et al. \(2022\)](#)).

In Section 2 we present the model, the latent Markov process, explain the graph properties, establish asymptotic results on sparsity and power-law and present a simulation algorithm. Section 3 describes a tractable approximation for the inference procedure, and in Section 4 we validate its use with synthetic data and then apply our method to a real-world graph. Empirical results show that dynSNetOC is able to recover the time-evolving communities while faithfully reproducing sparse connectivity and heavy-tailed degree distributions, while competitor models cannot capture all desirable properties. To the best of our knowledge, indeed, ours is the only proposal able to accommodate all four characteristics together.

2 Our model

2.1 Representation of a graph as a point process

[Caron & Fox \(2017\)](#) proposed an alternative framework for statistical network modelling, based on representing the graph as a point process. Specifically, a graph is modeled as an

exchangeable random measure on the plane where each node is embedded at some location $\theta_i \in \mathbb{R}_+$. A directed multigraph is represented by an atomic measure on the plane

$$N = \sum_{i,j} n_{ij} \delta_{(\theta_i, \theta_j)},$$

where n_{ij} is the number of directed edges from node i to j . The links are Poisson distributed

$$n_{ij} | (w_\ell)_{\ell=1,2,\dots} \sim \text{Poisson}(w_i w_j), \quad i \neq j$$

where the weights (w_i) represent node latent variables that makes it more or less prone to form connections. The weights and locations (w_i, θ_i) are draws from a Poisson process on $(0, \infty) \times \mathbb{R}_+$ defined by a mean measure $\nu(dw, d\theta) = \rho(dw)\lambda(d\theta)$, where λ is the Lebesgue measure and ρ is a σ -finite measure on \mathbb{R}_+ , concentrated on $\mathbb{R}_+ \setminus \{0\}$, which satisfies $\int_{\mathbb{R}_+} \min(1, w) \rho(dw) < \infty$. Under the prescribed conditions, the weights and locations (w_i, θ_i) are described by a completely random measure (CRM) (Kingman 1993) on \mathbb{R}_+ :

$$W = \sum_{i=1}^{\infty} w_i \delta_{\theta_i}, \quad W \sim \text{CRM}(\rho, \lambda).$$

More on the CRM construction and the properties of exchangeability are given in Caron & Fox (2017). Then, a directed graph N is generated from a Poisson process $N \mid W \sim \text{Poisson}(W \times W)$. The properties of the Lévy measure ρ will define the sparsity/density of the graph and other asymptotic properties of the graph. Therefore, its choice will be pivotal to the graph construction, as we will prove in section 2.4. If $\int_0^\infty \rho(dw) = \infty$, there are an infinite number of jumps in any finite interval and the CRM is said to have infinite activity. Otherwise, the number of jumps is finite almost surely and the CRM has finite activity.

2.2 Construction

Our proposed model dynSNetOC extends the overlapping community model of Todeschini et al. (2020) to the case where the nodes' affiliation scores to the communities evolve over

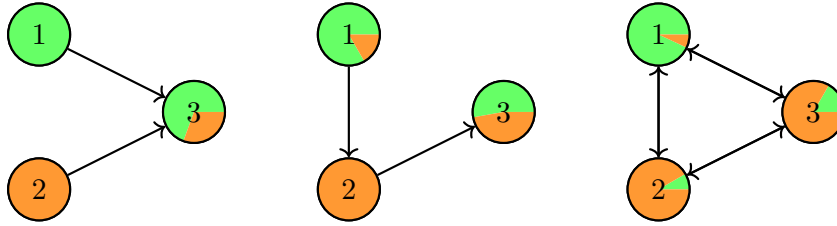


Figure 1: Snapshots of a graph with 3 nodes and 3 timesteps. There are 2 latent communities (green and orange), and each node is colored according to its affiliations.

time following a latent Markov process. In this way, we generalize the dynamic mixed membership stochastic blockmodel model to the sparse and power-law regime. Before giving a mathematical formulation, we demonstrate graphically how our model looks like. Figure 1 illustrates a toy example of our model formulation where there are 3 nodes, 3 timesteps and 2 communities, shown in green and orange. The arrows between the nodes show the directed links from one node to another and, as shown, these links change in time. The affiliations are shown in pie charts with green and orange colors corresponding to the proportion of affiliation to the two communities. At each timestep new edges appear or disappear between the nodes and the affiliations change too.

We now formally introduce the model, while the interpretation of the parameters is postponed to Section 2.3.1. We model graphs with p overlapping communities using vectors of completely random measures which evolve in time. We define $(W_1^{(t)}, \dots, W_p^{(t)})$ on \mathbb{R}_+^p , where each component is a homogeneous CRM with independent increments $W_k^{(t)} = \sum_{i=1}^{\infty} w_{ik}^{(t)} \delta_{\theta_i}$. The dynamic multigraph is thus described as follows:

$$\begin{aligned}
 W_k^{(t)} &= \sum_{i=1}^{\infty} w_{ik}^{(t)} \delta_{\theta_i} & (W_1^{(t)}, \dots, W_p^{(t)}) &\sim \text{CRM}(\rho^{(t)}, \lambda) \\
 N_k^{(t)} &= \sum_{i=1}^{\infty} \sum_{j=1}^{\infty} n_{ijk}^{(t)} \delta_{(\theta_i, \theta_j)} & N_k^{(t)} \mid W_k^{(t)} &\sim \text{Poisson}(W_k^{(t)} \times W_k^{(t)})
 \end{aligned} \tag{1}$$

where $n_{ijk}^{(t)}$ represent latent multiedges between nodes i and j within community k . The

overall observed process is

$$N^{(t)} = \sum_{i,j} n_{ij}^{(t)} \delta_{\theta_i, \theta_j}, \quad (2)$$

where $n_{ij}^{(t)} = \sum_{k=1}^p n_{ijk}^{(t)}$ is the total number of links in the pair i, j and $n_{ji}^{(t)} = n_{ij}^{(t)}$ according to

$$n_{ij}^{(t)} | (w_{\ell 1}^{(t)}, \dots, w_{\ell p}^{(t)})_{\ell=1,2,\dots} \sim \begin{cases} \text{Poisson} \left(2 \sum_{k=1}^p w_{ik}^{(t)} w_{jk}^{(t)} \right) & i \neq j \\ \text{Poisson} \left(\sum_{k=1}^p (w_{ik}^{(t)})^2 \right) & i = j \end{cases} \quad (3)$$

which is a non-negative Poisson factorization (Todeschini et al. 2020, Gopalan et al. 2015, Ball et al. 2011, Psorakis et al. 2011).

Although in this work we focus on multigraphs, note that if one is interested in the binary graph one could obtain it by setting a binary edge $z_{ij}^{(t)} = \mathbb{1}_{n_{ij}^{(t)} > 0}$ treating $n_{ij}^{(t)}$ as latent or, equivalently, using as link probability:

$$z_{ij}^{(t)} | (w_{\ell 1}^{(t)}, \dots, w_{\ell p}^{(t)})_{\ell=1,2,\dots} \sim \begin{cases} \text{Bernoulli} \left(1 - e^{-2 \sum_{k=1}^p w_{ik}^{(t)} w_{jk}^{(t)}} \right) & i \neq j \\ \text{Bernoulli} \left(1 - e^{-\sum_{k=1}^p (w_{ik}^{(t)})^2} \right) & i = j. \end{cases} \quad (4)$$

We construct the process so that marginally the vector of CRMs is a compound random measure (Griffin & Leisen 2017). The Lévy measure is

$$\rho^{(t)}(dw) = \int w_0^{-p} F^{(t)} \left(\frac{dw_1^{(t)}}{w_0}, \dots, \frac{dw_p^{(t)}}{w_0} \right) \rho_0(dw_0), \quad (5)$$

resulting in weights factorized as $w_{ik}^{(t)} = w_{i0} \beta_{ki}^{(t)}$, where the time dependence comes through the evolution of the CRM

$$W_k^{(t)} = \sum_{i=1}^{\infty} w_{0i} \beta_{ki}^{(t)} \delta_{\theta_i}. \quad (6)$$

Following Todeschini et al. (2020) we draw the weights w_{0i} choosing as Lévy measure ρ_0 the one of a generalized gamma process $\text{GGP}(\alpha, \sigma, \tau)$

$$\rho_0(dw_0) = \frac{1}{\Gamma(1-\sigma)} w_0^{-1-\sigma} e^{-w_0 \tau} dw_0 \quad (7)$$

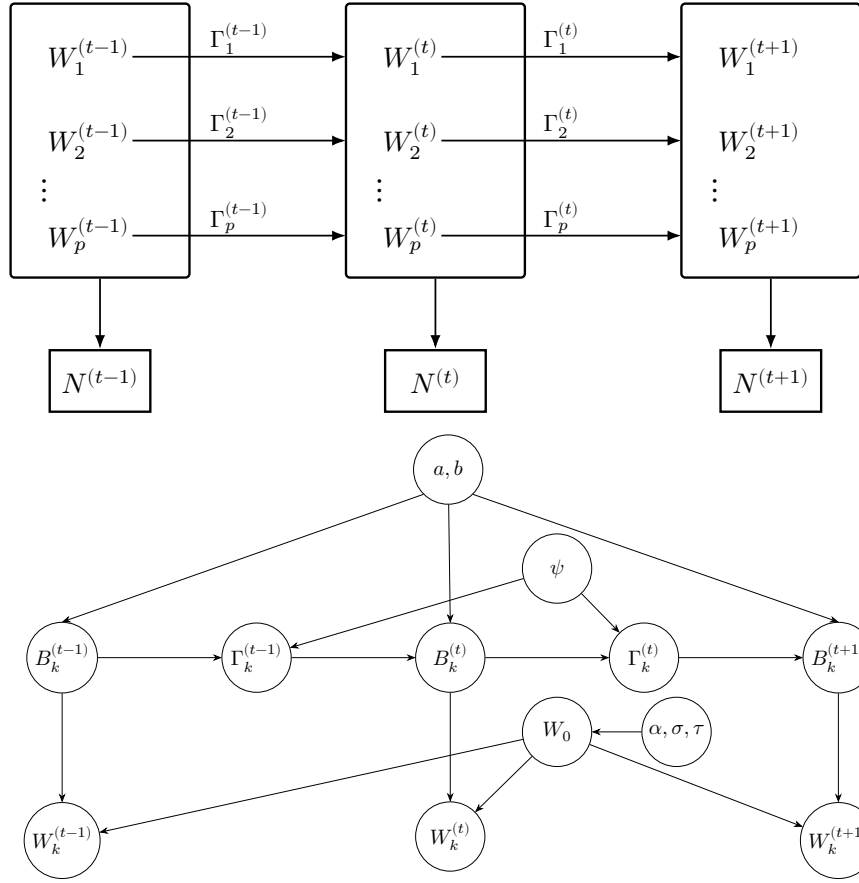


Figure 2: Structure of the model. Top: high level view of the latent Markov structure for all p measures. Bottom: Low level view of the latent structure in a given community k .

for $\sigma \in (\infty, 1), \tau > 0, \alpha > 0$. The scores $(\beta_k^{(t)})_{k=1}^p$ are drawn from p independent $\text{Gamma}(a_k, b_k)$ distributions for each timestep

$$F^{(t)}(d\beta_1^{(t)}, \dots, d\beta_p^{(t)}) = \prod_{k=1}^p F_k^{(t)}(d\beta_k^{(t)}) = \prod_{k=1}^p (\beta_k^{(t)})^{a_k-1} e^{-b_k \beta_k^{(t)}} \frac{(b_k)^{a_k}}{\Gamma(a_k)} d\beta_k^{(t)}. \quad (8)$$

This construction gives us a time-varying compound generalized gamma process (CGGP):

$$W^{(t)} = (W_1^{(t)}, \dots, W_p^{(t)}) \sim \text{CGGP}(\alpha, \sigma, \tau, F^{(t)}) \quad (9)$$

where $F^{(t)}$ is a product of Gamma distributions as shown in (8). We can also write this process as a combination of $W_0 = \sum_{i=1}^{\infty} w_{0i} \delta_{\theta_i} \sim \text{CRM}(\rho_0, \lambda)$ and the k -th score process $B_k^{(t)} = \sum_{i=1}^{\infty} \beta_{ki}^{(t)} \delta_{\theta_i}$. Their dependency will be explained below and they are shown graphically in Figure 2. Note that normalizing the scores of the nodes at each timestep we can

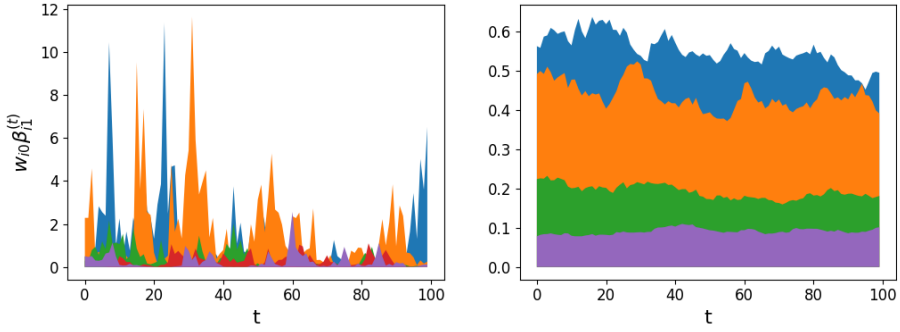


Figure 3: Temporal evolution of the weights of the first community of the 5 highest degree nodes from graphs generated from a CGGP model with $\sigma = 0.01, \tau = 1, \alpha = 2, p = 2, T = 100, a = b = (0.5, 0.5), \psi = 2$ (left) and $\psi = 2000$ (right).

visualize their percentage proportions of affiliations to each community as done in Figure 1.

2.3 A Markov process for the dynamic memberships

To have temporal dependency and evolution of community affiliations, the scores evolve stochastically over time following the ideas of Pitt & Walker (2012). The evolution is driven by augmentation variables $\gamma_{ki}^{(t)}$ giving rise to the p latent processes $\Gamma^{(t)} = (\Gamma_1^{(t)}, \dots, \Gamma_p^{(t)})$ with $\Gamma_k^{(t)} = \sum_{i=1}^{\infty} \gamma_{ki}^{(t)} \delta_{\theta_i}$. We construct them as below

$$\beta_{ki}^{(t)} \sim \text{Gamma}(a_k, b_k), \quad \gamma_{ki}^{(t)} | \beta_{ki}^{(t)} \sim \text{Gamma}(\psi, \beta_{ki}^{(t)}) \quad (10)$$

and hence the derived conditional is

$$\beta_{ki}^{(t)} | \gamma_{ki}^{(t)} \sim \text{Gamma}(a_k + \psi, \gamma_{ki}^{(t)} + b_k). \quad (11)$$

By taking the conditional law of $\beta_{ki}^{(t+1)} | \gamma_{ki}^{(t)}$ to be the same as that of $\beta_{ki}^{(t)} | \gamma_{ki}^{(t)}$, the marginals for the scores at time t and $t+1$ are the same $\text{Gamma}(a_k, b_k)$. The above ensures that the processes $B_k^{(t)} = \sum_{i=1}^{\infty} \beta_{ki}^{(t)} \delta_{\theta_i}$ and $W_k^{(t)} = \sum_{i=1}^{\infty} w_{ki}^{(t)} \delta_{\theta_i}$ have the same marginals, as explained in the next proposition. A high level graphical representation of the processes $W_k^{(t)}$ and $\Gamma_k^{(t)}$ is shown in Figure 2 (top).

Proposition 1 (Posterior of $W_k^{(t)}$ given $\Gamma^{(t)}$). Consider $W^{(t)}$ the Compound GGP on $(0, \infty) \times \Theta$ with intensity $\nu^{(t)}(dw) = \rho^{(t)}(dw) \lambda(d\theta)$ where the Lévy measure is defined in (5):

$$W^{(t)} \sim CGGP(\alpha, \sigma, \tau, F^{(t)}). \quad (12)$$

For each time t and community $k = 1, \dots, p$,

$$W_k^{(t)} = \sum_{i=1}^{\infty} \beta_{ki}^{(t)} w_{i0} \delta_{\theta_i}$$

with w_{i0} from (7) and $\beta_k^{(t)}, \gamma_{ki}^{(t)} \mid \beta_{ki}^{(t)}$ from (10). Then, the posterior $W_k^{(t)} | \Gamma_k^{(t)} = \sum \gamma_{ki}^{(t)} \delta_{\theta_i}$ is

$$W_k^{(t)} | \Gamma_k^{(t)} = \sum_{i=1}^{\infty} \tilde{\beta}_{ki}^{(t)} w_{0i} \delta_{\theta_i} \quad (13)$$

where

$$\tilde{\beta}_k^{(t)} \sim \tilde{F}_k^{(t)} = \text{Gamma}(a_k + \psi, b_k + \gamma_k^{(t)})$$

Therefore, the posterior is a compound GGP with score function $\tilde{F}^{(t)}$:

$$W^{(t)} | \Gamma^{(t)} \sim CGGP(\alpha, \sigma, \tau, \tilde{F}^{(t)}).$$

If we take $W_k^{(t+1)} | \Gamma_k^{(t)}$ to be distributed as in Equation (13), then $W_k^{(t+1)}$ and $W_k^{(t)}$ have the same marginal distributions. The dependence between $W_k^{(t)}, \Gamma_k^{(t)}, B_k^{(t)}, W_0$ and $N_k^{(t)}$ is shown in Figure 2 (bottom).

2.3.1 Interpretation of the parameters and hyperparameters

The hyperparameters α, σ, τ tune the overall properties of the graph (size, sparsity, degree distribution). The vectors $a = (a_1, \dots, a_p), b = (b_1, \dots, b_p)$ tune the distribution of the scores $\beta_{ki}^{(t)}, k = 1, \dots, p$, which represent the amount of affiliation of node i to community k at timestep t . w_{i0} can be seen as base sociabilities of each node (indeed, the link function is increasing in w_{i0}). They act as degree correction parameters, taking care of sparsity and

degree properties. Together with $(\beta_{ki}^{(t)})_k$ they define the sociability weights $w_{ik}^{(t)}$, which determine the number of links between nodes at time t . This construction can clearly model mixed memberships as the vectors $\beta_{ki}^{(t)}$ can have more than one nonzero values. The community scores evolve through a Markov process with the distribution of $\beta_{ki}^{(t+1)}$ depending on $\beta_{ki}^{(t)}$ through $\gamma_{ki}^{(t)}$. The parameter ψ governs the strength of correlation between timesteps, with larger ψ implying higher correlation across time and hence smoother changes in time as shown in Figure 3, where we generated graphs with the same hyperparameters except for ψ , which is $\psi = 2$ (left) and $\psi = 200$ (right).

2.4 Sparsity and Power-Law Properties

In this section, we prove some asymptotic results. To do so, we phrase our proposal in the more general setting of Caron et al. (2023), which studied the asymptotic properties of graphs generated by the so-called graphex process. Since generally $W_k^{(t)}(\mathbb{R}_+)$ and $N^{(t)}(\mathbb{R}_+^2)$ will be infinite, they will showcase an unbounded number of active nodes and edges. To model finite graphs and define an asymptotic process, we restrict the point process on a portion of the real line identified by those nodes satisfying $\theta \leq \alpha$ and discard nodes without connections, which in the case of infinite activity CRMs will be infinite even for the restricted process. The original, infinite dimensional graph, is obtained by studying the limit as α tends to infinity.

To proceed, we define the following summary statistics related to the restricted graphs (identified by the subscript α):

$$D_{\alpha i}^{(t)} := \frac{1}{2} \sum_{k \geq 1} N_{ik}^{(t)} \mathbb{1}_{\theta_k \leq \alpha}, \quad N_{\alpha}^{(t)} := \sum_{i=1}^{\infty} \mathbb{1}_{D_{\alpha i}^{(t)} \geq 1} \mathbb{1}_{\theta_i \leq \alpha} \quad (14)$$

which are respectively the number of connections of node i at time t and the number of nodes which display at least one connection at that timestep. We call these active nodes.

Switching from the multigraph to the simple¹ graph process, we define $Z_{ij}^{(t)} = 1$ if $N_{ij}^{(t)} > 0$.

Thus, we define

$$N_{\alpha j}^{(t)} := \sum_{i=1}^{\infty} \mathbb{1}_{\sum_j Z_{ij}^{(t)} = j} \mathbb{1}_{\theta_i \leq \alpha}, \quad E_{\alpha}^{(t)} := \frac{1}{2} \sum_{i \neq j} N_{ij}^{(t)} \mathbb{1}_{\theta_i \leq \alpha, \theta_j \leq \alpha} \quad (15)$$

as the number of active nodes with degree j as and the number of edges at time t respectively.

We recall that an increasing family of graphs with $N_{\alpha}^{(t)}$ active nodes and $E_{\alpha}^{(t)}$ edges is dense if $E_{\alpha}^{(t)} = \Theta((N_{\alpha}^{(t)})^2)$ and sparse if $E_{\alpha}^{(t)} = o((N_{\alpha}^{(t)})^2)$ as t grows to infinity. We can now prove the following propositions on sparsity and degree distribution.

Proposition 2 (Sparsity). *Let $N_{\alpha}^{(t)}$ and $E_{\alpha}^{(t)}$ be respectively the number of active nodes and edges at time t . As α tends to infinity and for every t ,*

$$E_{\alpha}^{(t)} \asymp \begin{cases} (N_{\alpha}^{(t)})^{2/(1+\sigma)} & \text{for } \sigma \in (0, 1) \\ (N_{\alpha}^{(t)})^2 / \log(N_{\alpha}^{(t)})^2 & \text{for } \sigma = 0 \\ (N_{\alpha}^{(t)})^2 & \text{for } \sigma < 0. \end{cases}$$

This result implies that for $\sigma < 0$ the resulting asymptotic graph is dense, for $\sigma \in (0, 1)$ it is sparse and for $\sigma = 0$ a transition regime known as almost density. It is also worth noting that a distinction on the sparsity and density could be obtained also by applying Proposition 1 of [Todeschini et al. \(2020\)](#), which proves that a finite activity CRM gives dense graphs, while an infinite activity CRM sparse graphs. Indeed, $\sigma \in (0, 1)$ and $\sigma < 0$ characterize respectively infinite and finite activity GGPs. Our proposition 2 here is stronger since it characterizes exactly the rates of growth of the edges as a function of the number of nodes.

Proposition 3 (Degree distribution). *Let $N_{\alpha}^{(t)}$ be the number of nodes at time t for the graph restricted at α , and $N_{\alpha, j}^{(t)}$ be the number of nodes with degree $j \geq 1$ at time t . As α*

¹A simple graph is a binary, undirected, graph with no self-loops.

tends to infinity and $\sigma \in (0, 1)$

$$\frac{C_1}{C_2} \frac{\sigma \Gamma(j - \sigma)}{j! \Gamma(1 - \sigma)} \leq \lim_{\alpha \rightarrow \infty} \frac{N_{\alpha j}^{(t)}}{N_{\alpha}^{(t)}} \leq \frac{C_2}{C_1} \frac{\sigma \Gamma(j - \sigma)}{j! \Gamma(1 - \sigma)}, \quad \text{for } j \geq 1 \quad (16)$$

where C_1, C_2 are positive real numbers. For $\sigma \leq 0$,

$$\frac{N_{\alpha j}^{(t)}}{N_{\alpha}^{(t)}} \rightarrow 0, \quad \text{for } j \geq 1$$

almost surely as α tends to infinity.

We can rewrite (16) using the fact that for j large $\frac{\sigma \Gamma(j - \sigma)}{j! \Gamma(1 - \sigma)} \sim \frac{\sigma}{\Gamma(1 - \sigma)} j^{-\sigma-1}$ and therefore for $\sigma \in (0, 1)$ the asymptotic graph displays a power-law degree distribution with exponent $1 + \sigma$ for large degrees. For the proofs of Propositions (2) and (3) see Section 6.1 of the Supplementary.

2.5 Simulation

The hierarchical nature of the model in (1) suggests a (brute force) simulation as below.

1. Sample $(w_{i0}, \theta)_{i=1,2,\dots}$ from a Poisson process with mean measure

$\rho_0(dw_{01}, \dots, dw_{0p}) \lambda(d\theta) 1_{\theta \in [0, \alpha]}$ and construct $\beta^{(t)}, \gamma^{(t)}$ for $t = 1, \dots, T$ from (10).

2. For each pair of nodes sample $n_{ij}^{(t)}$ from (3).

As explained in [Todeschini et al. \(2020\)](#) and [Caron & Fox \(2017\)](#) this has several challenges. In step 1. the measure is infinite and needs to be truncated at some threshold ϵ to generate a finite number of weights above ϵ . The truncation affects the w_0 s which would be sampled from the truncated measure ρ_0^ϵ . Equation (5) becomes $\rho_\epsilon^{(t)}(dw^{(t)}) = \int_\epsilon^\infty w_0^{-p} F^{(t)}\left(\frac{dw_1^{(t)}}{w_0}, \dots, \frac{dw_p^{(t)}}{w_0}\right) \rho_0(dw_0)$ and $\int_{\mathbb{R}_+^p} \rho_\epsilon^{(t)}(dw_1^{(t)}, \dots, dw_p^{(t)}) < \infty$, indicating that a smaller ϵ would lead to a better approximation. Secondly, in 2. we need to consider all pairs of nodes, which is $O(N^2)$ for N nodes. We therefore expand on [Todeschini et al. \(2020\)](#) and suggest the following, faster simulation scheme.

Simulation Algorithm

1. Sample the full set of parameters:

(a) Sample $(w_{i0}, \theta_i)_{1 \leq i \leq N}$ from a Poisson process with mean measure $\rho_0(dw_0)\lambda(d\theta)1_{\{w_0 > \epsilon, \theta \in [0, \alpha]\}}$, giving rise to a finite number of nodes L .

(b) For $t = 1, \dots, T$ sample $(\beta_{ki}^{(t)})_{1 \leq i \leq L, 1 \leq k \leq p}$ through the auxiliary variables $(\gamma_{ik}^{(t)})_{1 \leq i \leq L, 1 \leq k \leq p}$ from (10) (note that $\gamma_{ik}^{(t)}$ go up to $T - 1$ and not T).

These give rise to $w_{ik}^{(t)} = w_{i0}\beta_{ki}^{(t)}$, the corresponding measure $W_{k,\alpha}^{\epsilon(t)} = \sum_{i=1}^L w_{ik}^{(t)}\delta_{\theta_i}$ and their total masses $W_{k,\alpha}^{*\epsilon(t)} = \sum_{i=1}^L w_{ik}^{(t)}$, for $k = 1, \dots, p$.

2. For each $t = 1, \dots, T$ sample a graph:

(a) For $k = 1, \dots, p$ sample the total number of multiedges

$$N_{k,\alpha}^{\epsilon(t)} \mid W_{k,\alpha}^{*\epsilon(t)} \stackrel{\text{ind}}{\sim} \text{Poisson}((W_{k,\alpha}^{*\epsilon(t)})^2)$$

(b) For $k = 1, \dots, p$ and $\ell = 1, \dots, N_{k,\alpha}^{\epsilon(t)}$ sample the sender and receiver nodes

$$U_{k\ell j}^{(t)} \mid W_{k,\alpha}^{\epsilon(t)} \stackrel{\text{ind}}{\sim} W_{k,\alpha}^{\epsilon(t)}/W_{k,\alpha}^{*\epsilon(t)} \text{ for } j = 1, 2.$$

(c) Obtain the multigraph $N_{k,\alpha}^{\epsilon(t)} = \sum_{\ell=1}^{N_{k,\alpha}^{\epsilon(t)}} \delta_{U_{k\ell 1}^{(t)}, U_{k\ell 2}^{(t)}}$ per community k and sum over communities $N_{\alpha}^{\epsilon(t)} = \sum_{k=1}^p N_{k,\alpha}^{\epsilon(t)}$.

3 Inference

Assume that we observe multiple connections over time between a set of N_{α} nodes. Note that not all nodes appear in all timesteps, hence the observed numbers of nodes with at least one connection per timestep are denoted by the overlapping sets $N_{1,\alpha}, \dots, N_{T,\alpha}$ and we denote by N_{α} the union of them. We denote our observed data as $\mathcal{D} = \{(n_{ij}^{(1)})_{1 \leq i,j \leq N_{\alpha}}, \dots, (n_{ij}^{(T)})_{1 \leq i,j \leq N_{\alpha}}\}$, where at each timestep, some nodes might be of zero degree as explained above. Our goal is to infer the set of positive parameters $(w_{i1}^{(t)}, \dots, w_{ip}^{(t)})_{i=1, \dots, N_{\alpha}}$ for $t = 1, \dots, T$. These depend on the hyperparameters

$\xi = (\alpha, \sigma, \tau, \psi, a = (a_1, \dots, a_p), b = (b_1, \dots, b_p))$ of the model and the transition variables $(\gamma_{i1}^{(t)}, \dots, \gamma_{ip}^{(t)})_{i=1, \dots, N_\alpha}$. Note that we will not attempt to estimate the node locations $(\theta_i)_i$ as they are not likelihood identifiable. If one considers the model using the infinite activity GGP, then they should also estimate the positive parameters that are associated with nodes with no connections (that do not appear at all in the set of N_α nodes). These are only identifiable through their sum which we can be denoted as $(\tilde{W}_1^{(t)}, \dots, \tilde{W}_p^{(t)})$. Therefore the full posterior would be

$$p\left((\xi, w_{i1}^{(t)}, \dots, w_{ip}^{(t)}, \gamma_{i1}^{(t)}, \dots, \gamma_{ip}^{(t)}, W_1^{(t)}, \dots, \tilde{W}_p^{(t)})_{i=1, \dots, N_\alpha, t=1, \dots, T} | n^{(1)}, \dots, n^{(T)}\right),$$

where $n^{(t)} = (n_{ij}^{(t)})_{1 \leq i, j \leq N_\alpha}$. Various approaches can be taken for inference, such as maximum likelihood estimation or Bayesian inference either with MCMC sampling or a variational approximation. An algorithm for Bayesian inference with MCMC sampling can be devised by adapting the ideas of [Todeschini et al. \(2020\)](#) to the dynamic case. Instead of considering exact inference for the GGP prior, we rely on the proposal by [Lee et al. \(2023\)](#) to use as finite-dimensional independent and identically distributed approximation the exponentially tilted BFRY distribution (etBFRY)

$$w_{0i} \stackrel{\text{iid}}{\sim} \text{etBFRY}(\alpha/L, \tau, \sigma), \text{ for } i = 1, \dots, L \quad (17)$$

with density

$$g_{\alpha, L, \tau, \sigma}(w) = \frac{\sigma w^{-1-\sigma} e^{-\tau w} (1 - e^{-(\sigma L/\alpha)^{1/\sigma} w})}{\Gamma(1-\sigma) \{(\tau + (\sigma L/\alpha)^{1/\sigma})^\sigma - \tau^\sigma\}}. \quad (18)$$

As proved in [Lee et al. \(2023\)](#), the etBFRY distribution is guaranteed to converge to a GGP as the truncation level L approaches infinity: $\text{etBFRY}(\alpha/L, \tau, \sigma) \xrightarrow{d} \text{GGP}(\alpha, \sigma, \tau)$. Note that the truncation level L has to be bigger than the total number of active nodes N_α .

Approximate Posterior. The desired approximate posterior is

$$p\left(\xi, (w_{i1}^{(t)}, \dots, w_{ip}^{(t)}, \gamma_{i1}^{(t)}, \dots, \gamma_{ip}^{(t)})_{i=1, \dots, L, t=1, \dots, T} | N^{(1)}, \dots, N^{(T)}\right).$$

Considering a certain timestep t we can write

$$\begin{aligned} & p((w_{0i}, \beta_{1i}^{(t)}, \dots, \beta_{pi}^{(t)}, \gamma_{1i}^{(t)}, \dots, \gamma_{pi}^{(t)}, \gamma_{1i}^{(t-1)}, \dots, \gamma_{pi}^{(t-1)})_{i=1}^L, \xi | (n_{ij}^{(t)})_{i,j=1}^L) \\ & \propto p((n_{ij}^{(t)})_{i,j=1}^L | (w_{0i}, \beta_{1i}^{(t)}, \dots, \beta_{pi}^{(t)})_{i=1}^L) p((w_{0i})_{i=1}^L) p((\beta_{1i}^{(t)}, \dots, \beta_{pi}^{(t)})_{i=1}^L | (\gamma_{1i}^{(t-1)}, \dots, \gamma_{pi}^{(t-1)})_{i=1}^L) p(\xi) \end{aligned}$$

Using Bayes rule and (10), (11) we can compute $p((\beta_{ki}^{(t)})_{i=1}^L | (\gamma_{1i}^{(t-1)}, \dots, \gamma_{pi}^{(t-1)})_{i=1}^L) \propto p(\gamma_{ki}^{(t)} | \beta_{ki}^{(t)}) p(\beta_{ki}^{(t)} | \gamma_{ki}^{(t-1)})$ which is recognized as a Gamma random variable

$$\beta_{ki}^{(t)} | \gamma_{ki}^{(t-1)}, \gamma_{ki}^{(t)} \sim \text{Gamma} \left(a_k + 2\psi, \gamma_{ki}^{(t)} + \gamma_{ki}^{(t-1)} + b_k \right). \quad (19)$$

Note that (19) is only true for $t > 1$, since $\gamma_{ki}^{(0)}$ is not defined and for $t = 1$ $p(\beta_{ik}^{(1)} | \gamma_{ki}^{(0)}, \gamma_{ki}^{(1)}) \sim p(\beta_{ik}^{(1)} | \gamma_{ki}^{(1)})$ is given by Equation (11). Therefore, the full posterior at t is

$$\begin{aligned} & \log p((w_{0i}, \beta_{1i}^{(t)}, \dots, \beta_{pi}^{(t)}, \gamma_{1i}^{(t)}, \dots, \gamma_{pi}^{(t)}, \gamma_{1i}^{(t-1)}, \dots, \gamma_{pi}^{(t-1)})_{i=1}^L, \xi | (n_{ij}^{(t)})_{i,j=1}^L) \\ & \propto \log p((n_{ij}^{(t)})_{i,j=1}^L | (w_{0i}, \beta_{1i}^{(t)}, \dots, \beta_{pi}^{(t)})_{i=1}^L) + \log p((w_{0i})_{i=1}^L) \\ & \quad + \sum_k \log p(\beta_{ki}^{(t)})_{i=1}^L | (\gamma_{ki}^{(t)}, \gamma_{ki}^{(t-1)})_{i=1}^L + \log p(\xi) \\ & \propto \left[\sum_{i=1}^L \sum_{j=1}^L \log \text{Poisson} \left(n_{ij}^{(t)}; w_{0i} w_{j0} \sum_k \beta_{ki}^{(t)} \beta_{jk}^{(t)} \right) \right] \\ & \quad + \left[\sum_{i=1}^L \left(\log \text{BFRY}(w_{0i}; \alpha/L, \tau, \sigma) + \sum_k \log p(\beta_{ki}^{(t)} | \gamma_{ki}^{(t-1)}, \gamma_{ki}^{(t)}) \right) \right] + \log p(\xi). \end{aligned} \quad (20)$$

A more detailed version of the posterior is found in Section 6.2 of the Supplementary . Our goal is to perform Bayesian inference using MCMC aiming to approximate the posterior distribution in (20). An inference scheme can be devised extending ideas from [Todeschini et al. \(2020\)](#) and [Naik et al. \(2022\)](#) and considering HMC updates for the weights. In this work instead we use the NUTS ([Hoffman & Gelman 2014](#)) algorithm within the probabilistic language NumPyro ([Phan et al. 2019](#)).

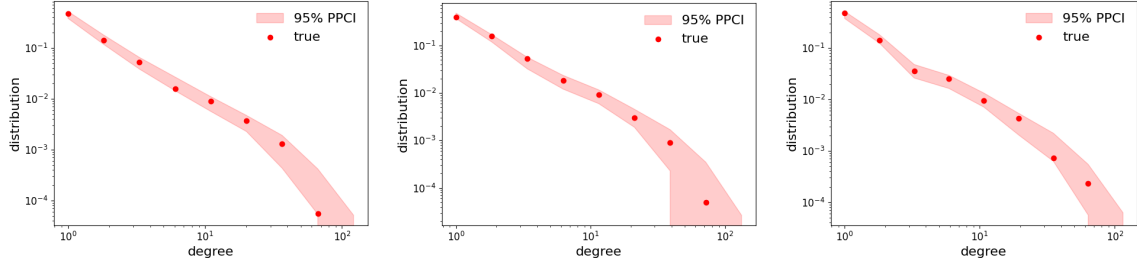


Figure 4: Degree distribution in log-log scale for the synthetic dataset in $t = 1$ (left), $t = 2$ (middle), $t = 3$ (right). Empirical degree in red dots, and 95% PPCI in the shaded region.

4 Experiments

4.1 Synthetic Experiment - validation of the approximation

In this section we first aim to validate our proposed approximation inference approach. We study the performance of the approximate inference on a synthetic dataset generated from the infinite Bayesian nonparametric model (see Section 2.5). We generate an undirected multigraph for $T = 3, p = 2$ with parameters $\alpha = 60, \sigma = 0.2, \tau = 1, \psi = 5, a = (1, 1), b = (1, 2)$. To generate the graph we used a threshold $\epsilon = 0.0001$. The synthetic graph has 1258 nodes of which the active nodes are 327 at $t = 1$, 330 at $t = 2$ and 321 at $t = 3$. We set $L = 1258$ and assume a positive Halfnormal prior on all unknown hyperparameters ξ . To assess convergence we inspect the trace plots of the two MCMC chains and give the plots of the hyperparameters $\alpha, \sigma, \psi, a, b$ in Figure 12 in Section 6.3 of the Supplementary. Regarding the parameters, namely the sociability weights w_{0i} and scores $\beta_{ki}^{(t)}$ are well recovered. Specifically, we obtained 96% coverage in the sociability weights and 95% in the scores (on average from the two chains). Additionally, we show the scores for a set of high degree nodes. In Figure 5 we show their true value (red dots) and 95% credible intervals (CI) in the shaded vertical bars for community 1 (left) and 2 (right). As the plot suggests, the algorithm recovers well the score values for each community. Note that in our model and also more broadly in SBMs, identifiability can be obtained up to label

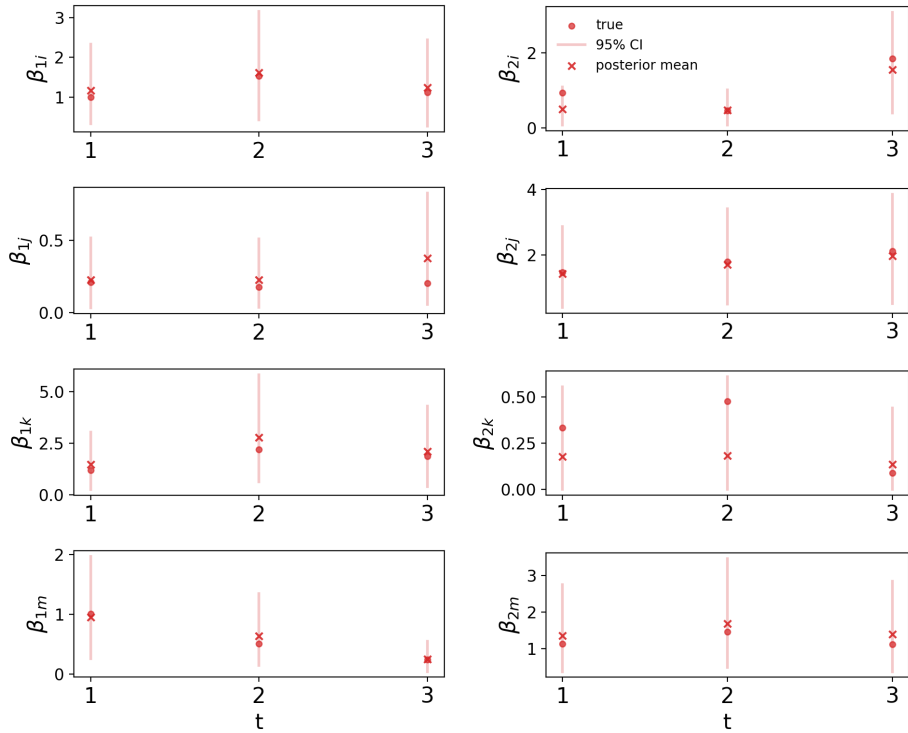


Figure 5: Temporal evolution of the scores for $t = 1, 2, 3$ for four high degree nodes (named i, j, k, m) of the network simulated from the CGGP model. True scores are in dots, and 95% CI in the vertical bars for community 1 (left) and community 2 (right).

switching of the communities, across timesteps. Hence caution is needed to interpret the order of the communities. To further assess model fit, we generate 500 graphs from the posterior predictive distribution. As shown in Figure 4, the shaded region, which is the 95% posterior predictive credible interval (PPCI) of the degree distribution, covers well the true empirical degree distribution. All together, these results mean that our model can capture well the power-law nature of such sparse graphs and in general recover the ground truth even when using an approximated inference.

4.2 Reuters Terror Dataset

Data Description. We now run our model to learn the dynamic evolution of the latent communities of a real-world network, being the Reuters terrorist dataset. This is

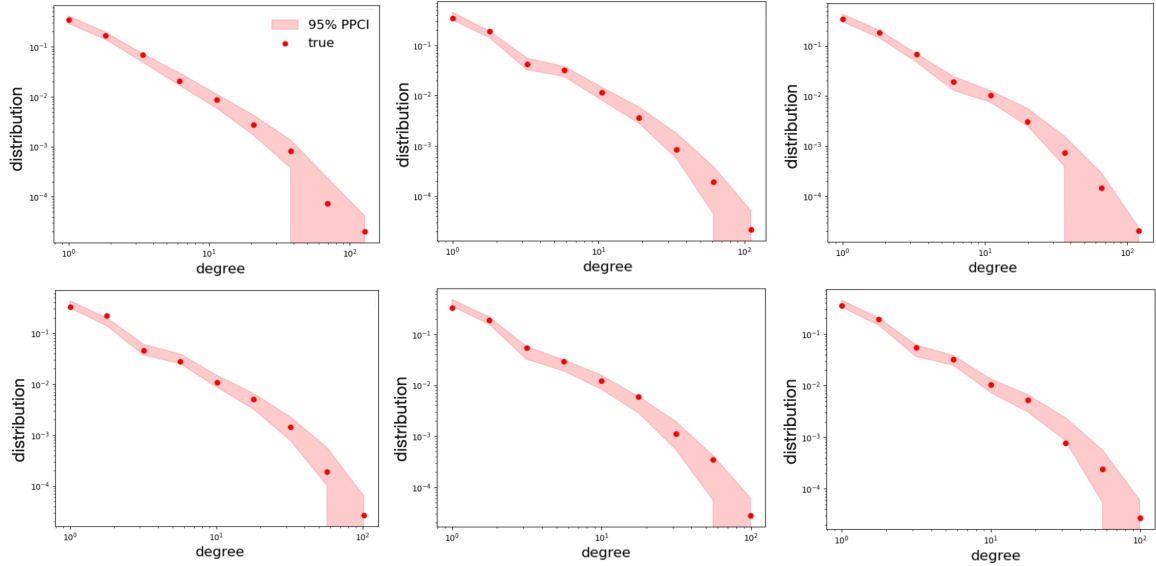


Figure 6: Degree distribution in log-log scale for reuters for $t = 1, 2, 3$ (top row) and $t = 4, 5, 6$ (bottom row). Empirical degree in red dots, and 95% PPCI in the shaded region.

a data set from the Reuters news agency concerning the 09/11/01 attack in the US. It is based on all stories published from 09/11/01 to 11/15/01, aggregated and shortened for our purposes. We aggregate the data from days into weeks and use the first $T = 6$ weeks after the attack. Nodes are words and edges represent co-occurrence of words in a sentence, creating a undirected multigraph. Not all words are present at each week, and only around 50% of the nodes are active at each timesteps. Specifically, the numbers of active nodes are $(468, 525, 501, 474, 471, 525)$. Empirical sparsity² at each timestep is $(0.02, 0.01, 0.01, 0.02, 0.02, 0.01)$, which indicates that the graphs are sparse. Our data consists of 6 sparse graphs of $L = 1200$ nodes where connections in the graph change in every timestep. The empirical degree distribution in each time is power-law, giving linear log-log degree distribution plots as shown by the red dots in Figure 6.

Inference. We run the NUTS algorithm on the data in order to estimate the unknown parameters and hyperparameters. We assume a vague positive Halfnormal prior on the

²measured as number of edges divided by the square of number of active nodes

Table 1: A high level view of representative words for each community for the 6 weeks.

Community	Representative words
‘Afghanistan’	Taliban, Al-Qaeda, Bin laden, Afghanistan
‘anthrax’	office, post, security, senate, senator, newspaper, sample, Brokaw
‘attack’	pentagon, new york, plane, hijack, WTC, attack
‘political’	foreign minister, official, military, economy, financial
‘security’	passenger, federal, hijacker, airline, agent, FBI, man

unknown hyperparameters, but for τ we fix its value to avoid identifiability issues following [Caron & Fox \(2017\)](#), [Todeschini et al. \(2020\)](#). We run one MCMC chain of 250,000 iterations of which 130,000 are discarded as burn-in. We give the trace plots of the identifiable parameters and the log-posterior (up to a constant) in Figure 13 in Section 6.4 of the Supplementary. The trace plots show good convergence of the algorithm. Based on previous work and the nature of the dataset, we expect the communities to represent topics or themes that appeared in the news following the 9-11 attack.

Previous work ([Li et al. 2009](#), [Dooley & Corman 2002](#)) justifies the existence of 5 observed communities throughout the $T = 6$ weeks, but not all of them appear at every single time point, as communities may appear or disappear. This is also suggested by [Li et al. \(2009\)](#) and we therefore expect to have 4 communities at each timestep, which suggests to run the model for $p = 4$.³

Note that setting $p = 4$ means that at any given timestep we have 4 communities, but since a community is just a container for a topic, the meaning of a community is allowed to change over time, with themes appearing and disappearing. Therefore, the total number

³Note that for exploration purposes we also ran our model for $p = 5$, but we concluded that $p = 4$ was of better fit and better interpretation, as suggested by the literature.

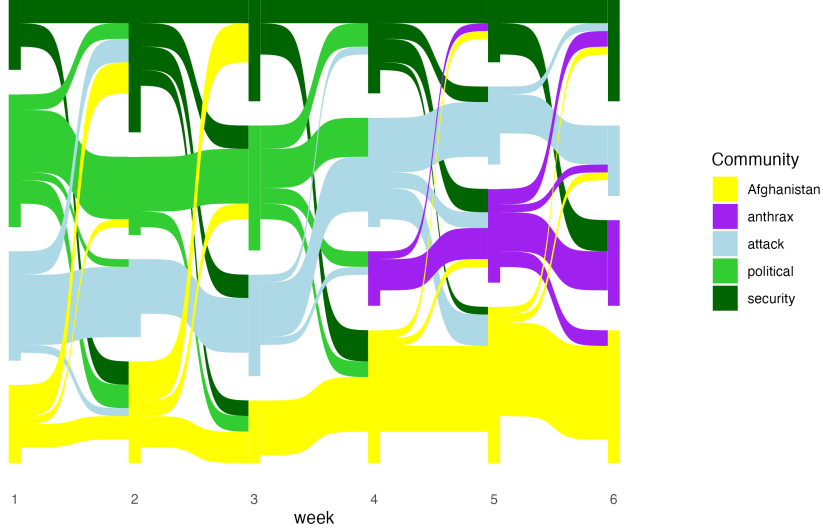


Figure 7: Sankey plot on the dynamic behavior of the words memberships for reuters using our model. Colors correspond to communities which evolve along the weeks.

of themes might be bigger than p . As we will show below, these topics evolve according to the historic events following the 9 – 11 attack, such as threat of war, political moves or health hazards. Cross referencing our results with the events that happened those days can verify the correctness of our approach.

From the MCMC inference we get estimates of all the parameters and hyperparameters. To assess the model fit, the posterior predictive degree distribution is shown in Figure 6 which shows that the 95% PPCI includes the empirical degree distribution.

Dynamic community interpretation. We estimate the community affiliations for all the words which we analyze and give below a detailed description of the discovered communities and their evolution. The communities we discover are ‘9-11 attack’, ‘Afghanistan’, ‘security’, ‘political response’, ‘anthrax’. As explained above, not all of them appear in all timesteps and words see their affiliation to the various communities varying with time. In Table 1 we give a high level summary of the 5 topics (communities). Words at the Table consider an overall picture of the communities from all 6 weeks.

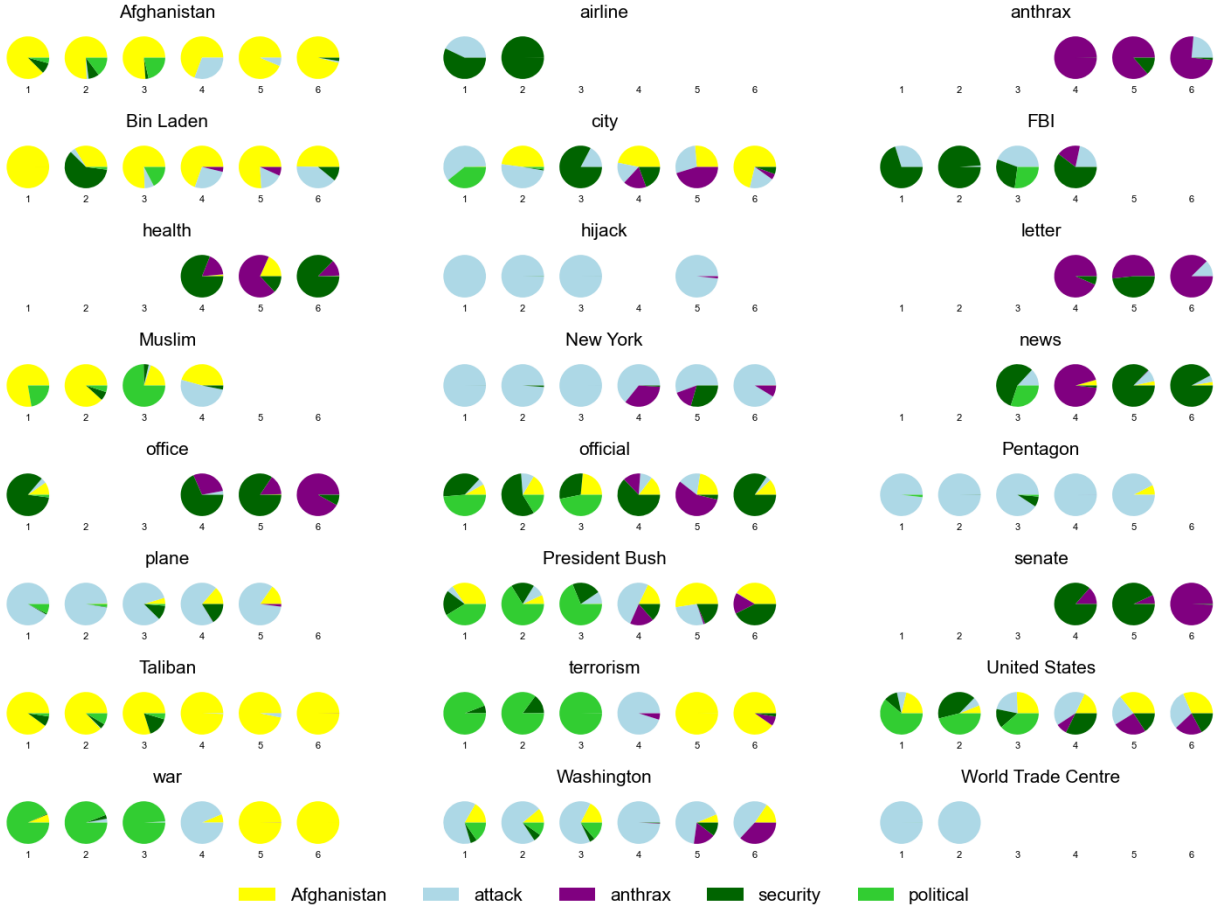


Figure 8: Pie charts with the % of community affiliations for some high degree words at each timestep using our model. If a word is not present at a certain timestep (i.e. it is not in the 50 highest degree nodes) then its pie plot doesn't exist.

We demonstrate the evolution of the communities along 6 weeks in Figure 7. The Sankey diagram shows the evolution of the dynamic behavior of the communities across the timesteps. The plot shows the affiliations of the 50 highest degree nodes for each week, assigning them to a community according to their highest affiliation. The thickness of the flow lines in the plot is proportional to the number of words in that community.

Since the highest degree words are not necessarily the same across timesteps, some of them do not flow to subsequent weeks or might appear later in the graph (represented by the vertical bars that do not move across timesteps). In Figure 8 we show the pie plots of the

dynamic memberships, from which one can appreciate the evolution of the communities through their principal words. Based on this information, we now describe the nature and dynamic evolution of the communities.

The community ‘attack’ describes the event of the attack which took place on 11th Sept 2001. Most of its words are associated with the WTC attack (e.g. *World Trade Centre, Pentagon, plane, hijacked*). On October 7 (week 4), the US invaded Afghanistan initiating what was known then as “war on terror”. Hence, some of the words that belonged to the community ‘political’ (*Bush, war, terrorism, US...*) on that week migrated towards ‘attack’ changing the interpretation of the community from a purely 9–11 attack to a mix with the attack to Afghanistan. We note how this switch also happens due to the necessity of having 4 communities per timestep, and the appearance of ‘anthrax’ implied the disappearance of one community. These same words move from week 5 to the ‘Afghanistan’ community.

Community ‘Afghanistan’ during the first three weeks is composed by the words related to the Taliban word (*Afghanistan, Taliban, Bin Laden and Muslim*) and after weeks 4 and 5 it grows including the aforementioned words related to the war in Afghanistan.

The community ‘political’ is represented by words explaining the political scene, which however is blended with the military and the financial spheres. Some representatives words are *foreign minister, official, war, terrorism*. In week 1 there is strong presence of financial words within political, such as *economy* or *financial*. As explained, ‘political’ ceases to exist on its own by week 4 and gets merged with ‘attack’. Some of its words are absorbed in others, and at the same time a new community appears at this time, named ‘anthrax’.

‘Anthrax’ appears when the first death due to the anthrax attacks was observed on October 5. Letters containing anthrax spores were mailed to media offices and political figures, leading to the illness of 22 people and the deaths of 5, according to the Federal Bureau of Investigation (FBI) and the Centers for Disease Control and Prevention (CDC). Top words

of are *case*, *antibiotic*, *spore*, *test*, *bacterium*, *news*, *anthrax*, *letter*, *deadly*. Note that also one of the top words is *Brokaw*, which is the name of an American NBC journalist who covered the event and also received a letter with the spore of anthrax. In weeks 5 and 6 we observe some words switching across ‘anthrax’ and ‘security’ and vice versa (*official*, *health*, *news*, *senate* which indicate the dual nature of those communities that both relate to health security. In the first weeks, ‘security’ is mostly related to air and state security, including words such as *passenger*, *airline* and *federal*, *agent*, *FBI*. In week 3 this community evolves around the event involving the journalist Yvonne Ridley, who was held captive by the Taliban in Afghanistan after the attacks but was later released and returned to the UK.

The Sankey diagram we can only represent thresholded affiliations to single communities, ignoring the overlap that our model allows. In order to see the multiple memberships for each word used we refer to Figure 8. For example, *president Bush* and *war* switch in weeks 3, 4 and 5 from ‘political response’ to ‘attack’ and then ‘Afghanistan’ as highlighted previously. From the pie plots, we can also appreciate how hard clustering is a crude representation of reality, since many of these words have a more nuanced belonging to various communities: *city*, which is affiliated to various communities, switches meaning by being first associated mostly to New York and then to the city of Kandahar in Afghanistan, one of the principal site of the US bombing in October 2001. In *letter*, *office*, *senate* and *health* we see both affiliations to ‘anthrax’ and ‘security’.

4.3 Comparisons

4.3.1 Sparse network with overlapping communities (SNetOC)

As a baseline, we fit the static overlapping community model of [Todeschini et al. \(2020\)](#) (SNetOC) on an aggregated static view of the graph, using the code provided by the authors. This model is designed to handle well sparsity and degree heterogeneity with overlapping

Table 2: Top representative words for each community under SNetOC with aggregated data from 6 weeks with $p = 5$.

Community	Representative words
‘attack’	plane, hijack, WTC, flight, airport, passenger, September, hijacker, jet, tower, pentagon, pilot
‘war on terror’	US, attack, Afghanistan, Bush, people, country, terrorism, war, Bin Laden, military, Washington, force, Al Quaeda, state, campaign, muslim, action
‘political’	security, bank, foreign, minister, airline, health, financial, business, Australian, committee, trade, German
‘anthrax’	anthrax, official, letter, New York, mail, test, office, building, news, case, capitol, FBI, bacterium, senate, antibiotic, post, hospital
‘Taliban’	Taliban, Kabul, city, Kandahar, tell, capital, reporter, Pakistani, mullah, southern, opposition, border, province, resident, Israeli

community structure. We run the model with $p = 5$ communities overall. We get point estimates of the weights using the minimum Bayes risk point estimate as done in the original paper and assign the words to their highest membership to get the communities as shown in Table 2. Taking the top representative words of each community we see that communities ‘anthrax’, ‘attack’ and ‘political’ are quite similar in meaning as in our case. We renamed our ‘Afghanistan’ and ‘security’ communities as ‘Taliban’ and ‘war on terror’ due to the words belonging to them. Using this static approach we cannot see words change communities, how the theme of a community evolves, appears or disappears, making it not possible to track any dynamic evolution. For example in our model, ‘attack’ is the ‘9-11’ attack but later on it acquires additional words regarding the attack in Afghanistan, whereas in the static model ‘attack’ only concerns words of ‘9-11 attack’. Another example is the community ‘security’ which in our model first is about airport and airline security

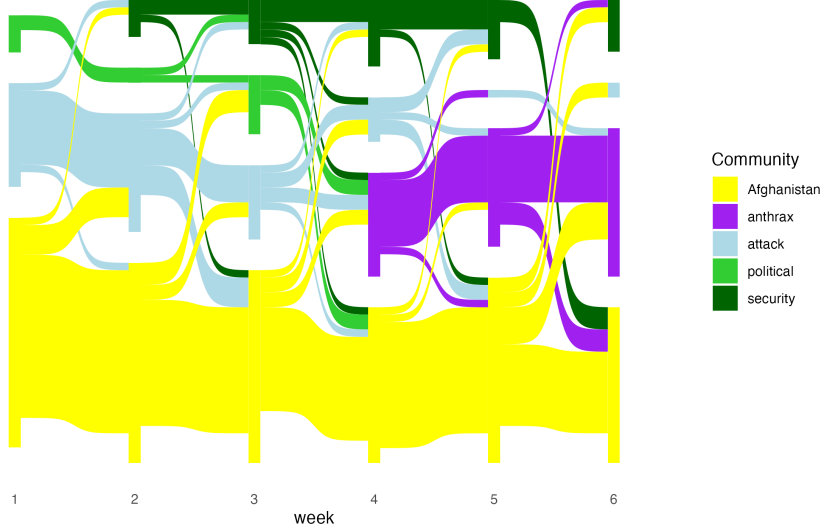


Figure 9: Sankey plot of weekly affiliation of representative words using SNetOC at each timestep with $p = 4$.

whereas later relates to health and state security. In the static case, we cannot see this evolution at all and in fact, security does not exist as a community on its own as it is blended with the rest.

4.3.2 Sparse network with overlapping communities (SNetOC) at each week

We run SNetOC at each timestep with $p = 4$. As expected, the posterior predictive degree distribution is good. There is a meaningful recovery of communities, but the model cannot track their evolution, since we have to estimate T different models. For example the words *war*, *Bush*, *terrorism*, *US* are throughout in community ‘Afghanistan’ and do not belong to ‘political’ as they do under our model (for $t = 1, 2, 3$). This shows that there is no meaningful mixing between these two communities. Similarly, there is less mixing between ‘security’ and ‘anthrax’ as the words *anthrax*, *health*, *letter* are affiliated with ‘anthrax’ but they do not pick up a ‘security’ component as they do in our case. The pie plots of the words are found in Section 6.5 of the Supplementary. The sankey plot is shown in Figure 9. It is evident that $p = 4$ is not the best choice. Indeed at week 1 there are only

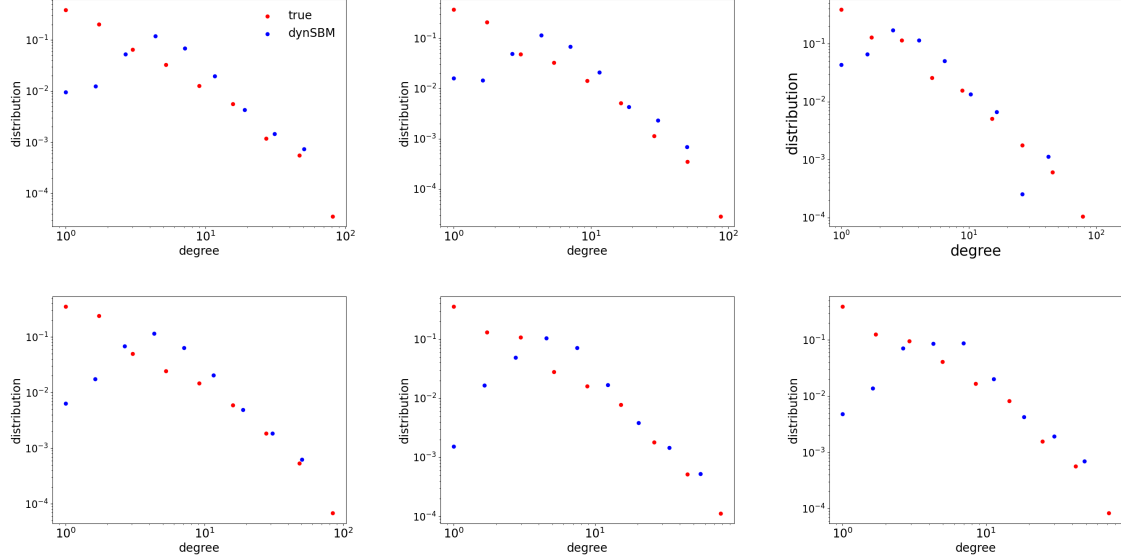


Figure 10: Degree distribution in log-log scale, empirical in red dots vs the degree distribution under dynSBM in blue dots for $t = 1, 2, 3$ (top row), and $t = 4, 5, 6$ (bottom row).

3 communities, one of which ('political') contains only 5 words, of which only 2 (*foreign* and *minister*) survive over the subsequent weeks. The vast majority of words belongs to the 'attack' community, which in the first 2-3 weeks is about the WTC attack. The rest of the words are in 'Afghanistan', which has a broader meaning than it had with our dynamic proposal, including words from the sphere of Taliban, terrorism, war, US (*United States, Bush, national*) and the political/financial worlds (*security, financial, coalition*). As time evolves, 'Afghanistan' and 'attack' tend to shrink and new communities arise, such as 'security' and 'anthrax'. 'Security' is a combination of national security coming from the attack to Afghanistan (*Taliban, foreign, Kabul, Kandahar, national, Pentagon*), airport security (*airport, plane*) and health security (*hospital*). In the last two weeks, again the results seem to suggest that $p = 3$ or $p = 2$ would provide a better fit.

Overall, SNetOC on the aggregated data from all timesteps provides interesting results for $p = 5$, but these do not carry out to similarly interpretable results when we separate the timesteps. It is evident that our proposal, which takes into account time dynamics,

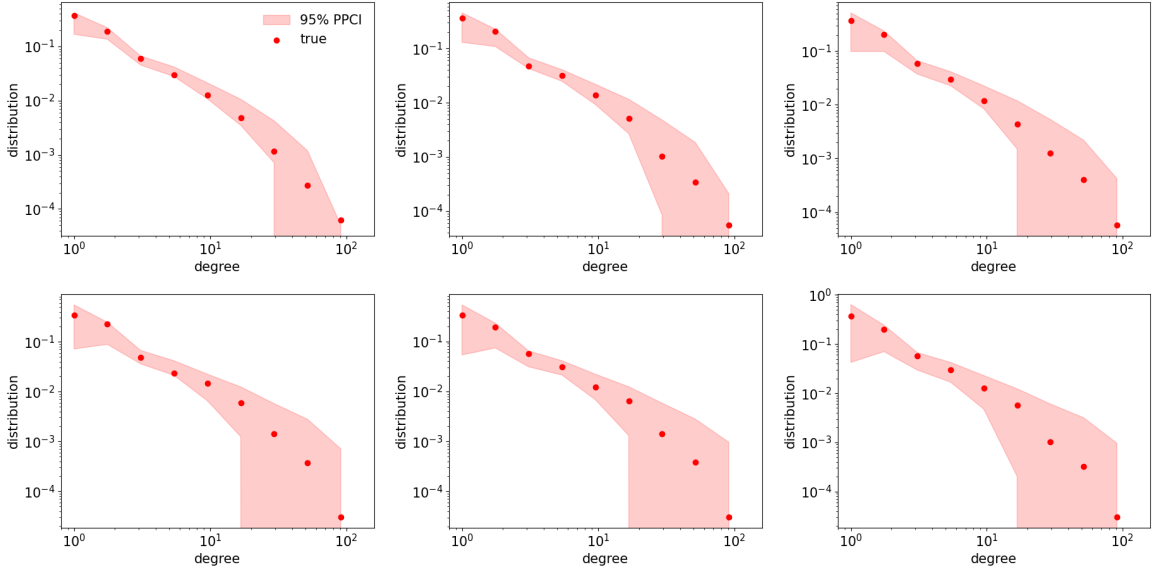


Figure 11: Degree distribution in log-log scale for dMMSB, empirical in red dots and 95% PPCI in shaded region for $t = 1, 2, 3$ (top row), and $t = 4, 5, 6$ (bottom row).

is able to better represent the evolution of communities through different meanings across timesteps. For example, through a semantic change of ‘attack’ from WTC to the attack to Afghanistan, or the change of ‘security’ from airport security to national security and then health security. With SNetOC, the ‘attack’ community loses strength over time, and ‘security’ appears in a weaker form (less words and without a clear semantic change, on the contrary a mix of concepts from the beginning).

4.3.3 Dynamic Stochastic Blockmodel

The Dynamic Stochastic Blockmodel (dynSBM) (Matias & Miele 2017b) is the celebrated temporal extension of the SBM where nodes have dynamic single memberships. The mathematical formulation of the model is found in Section 6.6 of the Supplementary. Parameter estimation is performed with a variational Expectation–Maximization (VEM) algorithm and the authors provide the R software (Matias & Miele 2017a). We run dynSBM on the binary graph with $p = 4$ and generate graphs from the posterior as shown in Figure 10.⁴

⁴We cannot provide similar uncertainty intervals for dynSBM in the same way as in our case.

Regarding the discovered communities, there is no meaningful thematic interpretation. Interestingly, at all timesteps, one of the communities has around 80% of the nodes. We believe that the poor fit is caused by the high sparsity of the connections and the scale-free degree distribution, which are not features handled by the dynSBM.

4.3.4 Dynamic Mixed Membership Stochastic Blockmodel

The Dynamic Mixed Membership Stochastic Blockmodel (dMMSB) [Xing et al. \(2010\)](#) is the extension of the SBM where nodes have dynamic mixed group memberships. The formulation is in Section [6.7](#) of Supplementary. Given the lack of software, we created code⁵ to implement the proposed EM algorithm. We run dMMSB on the binary graph with $p = 4$ and generate graphs from the posterior predictive, shown in Figure [11](#). The fit is better than dynSBM, but this comes at expense of the community structure. In fact, the block matrix is estimated to have a single non-zero entry on the diagonal with all off-diagonal elements set to zero, implying that all connections happen inside a single community. Hard-clustering the nodes shows that the only information used to assign words to communities is the degree: the only active community is made of the highest degree nodes. Overall, the estimated model fails to function as a community detection algorithm for this sparse dataset and only manages to model the degree heterogeneity of the data by using the community parameters.

5 Conclusion

We propose a Bayesian nonparametric model for dynamic evolution of communities in sparse graphs with power-law degree distribution. In this way, our work generalizes existing overlapping community models to the sparse and power-law regime and its applicability is

⁵<https://github.com/LaosAntreas/dMMSB>

demonstrated on a real-world graph. Future work could be the inclusion of covariates or an estimation of the number of communities.

Note. Regarding contributions, AL implemented and applied the code of dMMSB, contributed to our model’s code and performed the reuters’ data cleaning. Everything else was shared equally by XM and FP. The authors would like to thank François Caron for the insightful discussions.

References

Airoldi, E. M., Blei, D., Fienberg, S. E. & Xing, E. (2008), ‘Mixed membership stochastic blockmodels’, *The Journal of Machine Learning Research* **9**, 1981–2014.

Ball, B., Karrer, B. & Newman, M. E. J. (2011), ‘Efficient and principled method for detecting communities in networks’, *Physical Review E* **84**, 036103.

Borgs, C., Chayes, J., Cohn, H. & Holden, N. (2018), ‘Sparse exchangeable graphs and their limits via graphon processes’, *The Journal of Machine Learning Research* **18**(1), 1–71.

Caron, F. & Fox, E. (2017), ‘Sparse graphs using exchangeable random measures’, *Journal of the Royal Statistical Society Series B: Statistical Methodology* **79**(5), 1295–1366.

Caron, F., Panero, F. & Rousseau, J. (2023), ‘On sparsity, power-law, and clustering properties of graphex processes’, *Advances in Applied Probability* **55**(4), 1211–1253.

Dooley, K. J. & Corman, S. R. (2002), The dynamics of electronic media coverage, in B. S. Greenberg, ed., ‘Communication and Terrorism: Public and Media Responses to 9/11’, Hampton Press, Cresskill, NJ, pp. 121–135. Accessed in 2024.

Fortunato, S. (2010), ‘Community detection in graphs’, *Physics Reports* **486**(3-5), 75–174.

Fu, W., Song, L. & Xing, E. P. (2009), Dynamic mixed membership blockmodel for evolving networks, *in* ‘Proceedings of the 26th Annual International Conference on Machine Learning’, pp. 329–336.

Gopalan, P., Hofman, J. M. & Blei, D. M. (2015), Scalable Recommendation with Hierarchical Poisson Factorization, *in* ‘UAI’, pp. 326–335.

Griffin, J. E. & Leisen, F. (2017), ‘Compound random measures and their use in bayesian non-parametrics’, *Journal of the Royal Statistical Society Series B: Statistical Methodology* **79**(2), 525–545.

Herlau, T., Mørup, M. & Schmidt, M. (2013), Modeling Temporal Evolution and Multiscale Structure in Networks, *in* ‘Proceedings of the 30th International Conference on Machine Learning’, Proceedings of Machine Learning Research, PMLR, pp. 960–968.

Herlau, T., Schmidt, M. N. & Mørup, M. (2014), ‘Infinite-degree-corrected stochastic block model’, *Physical Review E* **90**(3), 032819.

Ho, Q., Song, L. & Xing, E. (2011), Evolving cluster mixed-membership blockmodel for time-evolving networks, *in* ‘Proceedings of the Fourteenth International Conference on Artificial Intelligence and Statistics’, pp. 342–350.

Hoff, P. D. (2009), ‘Multiplicative latent factor models for description and prediction of social networks’, *Computational Math. Organizational Theory* **15**, 261–272.

Hoff, P. D., Raftery, A. E. & Handcock, M. S. (2002), ‘Latent Space Approaches to Social Network Analysis’, *Journal of the American Statistical Association* **97**(460), 1090–1098.

Hoffman, M. D. & Gelman, A. (2014), ‘The no-u-turn sampler: Adaptively setting path lengths in hamiltonian monte carlo’, *Journal of Machine Learning Research* **15**, 1593–1623.

Ishiguro, K., Iwata, T., Ueda, N. & Tenenbaum, J. B. (2010), Dynamic infinite relational

model for time-varying relational data analysis, *in* ‘NIPS’, pp. 919–927.

Kallenberg, O. (1990), ‘Exchangeable random measures in the plane’, *Journal of Theoretical*

Probability **3**(1), 81–136.

Kang, X., Ganguly, A. & Kolaczyk, E. D. (2022), ‘Dynamic networks with multi-scale

temporal structure’, *Sankhya A* **84**(1), 218–260.

Kingman, J. (1993), *Poisson processes*, Vol. 3, Oxford University Press, USA.

Kolaczyk, E. D. (2009), *Statistical Analysis of Network Data: Methods and Models*,

Springer.

Lee, J., Minciardiou, X. & Caron, F. (2023), ‘A unified construction for series representa-

tions and finite approximations of completely random measures’, *Bernoulli* **29**(3), 2142–

2166.

Li, J., Cheung, W. K., Liu, J. & Li, C. (2009), On discovering community trends in social

networks, *in* ‘2009 IEEE/WIC/ACM International Joint Conference on Web Intelligence

and Intelligent Agent Technology’, Vol. 1, IEEE, pp. 230–237.

Lovász, L. (2013), *Large Networks and Graph Limits*, Vol. 60 of *Colloquium Publications*,

American Mathematical Society, Providence, RI.

Martinet, L.-E., Kramer, M., Viles, W., Perkins, L., Spencer, E., Chu, C., Cash, S. &

Kolaczyk, E. (2020), ‘Robust dynamic community detection with applications to human

brain functional networks’, *Nature communications* **11**(1), 1–13.

Matias, C. & Miele, V. (2017a), *dynsbm: Dynamic Stochastic Block Models*.

URL: <https://CRAN.R-project.org/package=dynsbm>

Matias, C. & Miele, V. (2017b), ‘Statistical clustering of temporal networks through a dynamic stochastic block model’, *Journal of the Royal Statistical Society Series B: Statistical Methodology* **79**(4), 1119–1141.

Naik, C., Caron, F., Rousseau, J., Teh, Y. W. & Palla, K. (2022), Bayesian nonparametrics for sparse dynamic networks, in ‘Machine Learning and Knowledge Discovery in Databases’, Springer, pp. 191–206.

Newman, M. (2010), *Networks: an Introduction*, OUP Oxford.

Newman, M. E. J. (2006), ‘Modularity and community structure in networks’, *Proceedings of the National Academy of Sciences* **103**(23), 8577–8582.

Orbánz, P. & Roy, D. M. (2015), ‘Bayesian Models of Graphs, Arrays and Other Exchangeable Random Structures’, *IEEE Transactions on Pattern Analysis and Machine Intelligence (PAMI)* **37**(2), 437–461.

Phan, D., Pradhan, N. & Jankowiak, M. (2019), ‘Composable effects for flexible and accelerated probabilistic programming in numpyro’, *arXiv preprint arXiv:1912.11554*.

URL: <https://arxiv.org/abs/1912.11554>

Pitt, M. K. & Walker, S. G. (2012), ‘Constructing stationary time series models using auxiliary variables with applications’, *Journal of the American Statistical Association* **100**(470), 554–564.

Psorakis, I., Roberts, S., Ebden, M. & Sheldon, B. (2011), ‘Overlapping community detection using bayesian non-negative matrix factorization’, *Physical Review E* **83**(6), 066114.

Ricci, F. Z., Guindani, M. & Sudderth, E. (2022), ‘Thinned random measures for sparse graphs with overlapping communities’, *Advances in Neural Information Processing Systems* **35**, 38162–38175.

Sarkar, P. & Moore, A. W. (2005), Dynamic social network analysis using latent space models, in ‘Proceedings of the 19th International Conference on Neural Information Processing Systems’, NIPS’05, MIT Press, Cambridge, MA, USA, p. 1145–1152.

Todeschini, A., Minciucou, X. & Caron, F. (2020), ‘Exchangeable random measures for sparse and modular graphs with overlapping communities’, *Journal of the Royal Statistical Society Series B: Statistical Methodology* **82**(2), 487–520.

Veitch, V. & Roy, D. M. (2015), ‘The Class of Random Graphs Arising from Exchangeable Random Measures’, *arXiv preprint arXiv:1512.03099* .

Wilson, J. D., Stevens, N. T. & Woodall, W. H. (2019), ‘Modeling and detecting change in temporal networks via the degree corrected stochastic block model’, *Quality and Reliability Engineering International* **35**(5), 1363–1378.

Wu, L., Cui, P., J., P. & Zhao, L. (2022), *Graph Neural Networks: Foundations, Frontiers, and Applications*, Springer.

Xing, E. P., Fu, W., Song, L. et al. (2010), ‘A state-space mixed membership blockmodel for dynamic network tomography’, *The Annals of Applied Statistics* **4**(2), 535–566.

Xu, A. & Zheng, X. (2009), Dynamic Social Network Analysis Using Latent Space Model and an Integrated Clustering Algorithm, in ‘2009 Eighth IEEE International Conference on Dependable, Autonomic and Secure Computing’, pp. 620–625.

Xu, K. S. & Hero, A. O. (2013), Dynamic stochastic blockmodels: Statistical models for time-evolving networks, in ‘International conference on social computing, behavioral-cultural modeling, and prediction’, Springer, pp. 201–210.

Xu, Z., Tresp, V., Yu, K. & Kriegel, H.-P. (2012), Infinite hidden relational models, in

‘Proceedings of the Twenty-Second Conference on Uncertainty in Artificial Intelligence’,
p. 544–551.

Yang, T., Chi, Y., Zhu, S., Gong, Y. & Jin, R. (2011), ‘Detecting communities and their evolutions in dynamic social networks—a bayesian approach’, *Machine learning* **82**(2), 157–189.

6 Supplementary

6.1 Proof of propositions 2 and 3

Proof. Propositions (2) and (3) follow from Remark 5 in [Caron et al. \(2023\)](#) upon noting that

$$1 - e^{-2 \sum_{k=1}^p w_{ki}^{(t)} w_{kj}^{(t)}} = 1 - e^{-2 w_{0i} w_{0j} \sum_{k=1}^p \beta_{ki}^{(t)} \beta_{kj}^{(t)}} = 1 - e^{\eta(w_{0i}, w_{0j}) \omega(\beta_i^{(t)}, \beta_j^{(t)})}$$

where $\omega(\beta_i^{(t)}, \beta_j^{(t)}) := \sum_{k=1}^p \beta_{ki}^{(t)} \beta_{kj}^{(t)}$ and $\eta(w_{0i}, w_{0j}) := 2 w_{0i} w_{0j}$. To map back to the notation of [Caron et al. \(2023\)](#) we note that w_{0i} can be obtained as $w_{0i} = \bar{\rho}_0^{-1}(\vartheta_i)$, with ρ_0 the Lévy measure of the generalized gamma process, $\bar{\rho}_0(x) = \int_x^\infty \rho_0(dy)$ its tail Lévy intensity and $(\vartheta_i)_{i \geq 1}$ random variables sampled from a unit-rate Poisson process. \square

6.2 Posterior distribution

The full posterior at t is

$$\begin{aligned}
& \log p(\mathbf{w}_0, \beta_1^{(t)}, \dots, \beta_p^{(t)}, \gamma_1^{(t)}, \dots, \gamma_p^{(t)}, \gamma_1^{(t-1)}, \dots, \gamma_p^{(t-1)}, \xi \mid \mathbf{n}^{(t)}) \\
& \propto \log p(\mathbf{n}^{(t)} \mid \mathbf{w}_0, \beta_1^{(t)}, \dots, \beta_p^{(t)}) + \log p(\mathbf{w}_0) + \sum_k \log p(\beta_k^{(t)} \mid \gamma_k^{(t)}, \gamma_k^{(t-1)}) + \log p(\xi) \\
& \propto \left[\sum_{i=1}^L \sum_{j=1}^L \log \text{Poisson} \left(n_{ij}^{(t)}; w_{0i} w_{j0} \sum_k \beta_{ki}^{(t)} \beta_{jk}^{(t)} \right) \right] \\
& \quad + \left[\sum_{i=1}^L \left(\log \text{BFRY}(w_{0i}; \alpha/L, \tau, \sigma) + \sum_k \log p(\beta_{ki}^{(t)} \mid \gamma_{ki}^{(t-1)}, \gamma_{ki}^{(t)}) \right) \right] + \log p(\xi) \\
& \propto \sum_{i=1}^L \left(m_{ti} \log \left(w_{0i} \sum_k \beta_{tki} \right) - (1 + \sigma) \log w_{0i} - \tau w_{0i} + \log(1 - e^{-(\sigma/\alpha)^{1/\sigma} w_{0i}}) \right. \\
& \quad \left. + \sum_{k=1}^p (a_k + \psi - 1 + \mathbb{1}_{t>1} \psi) \log \beta_{ki}^{(t)} - (b_k + \gamma^{(t)} + \mathbb{1}_{t>1} \gamma_k^{(t-1)}) \beta_{ki}^{(t)} \right. \\
& \quad \left. + (a_k + \psi + \mathbb{1}_{t>1} \psi) \log(b_k + \gamma^{(t)} + \mathbb{1}_{t>1} \gamma_k^{(t-1)}) - \Gamma(a_k + \psi + \mathbb{1}_{t>1} \psi) \right) \\
& \quad + \log \sigma - \log \Gamma(1 - \sigma) - \log \left((\tau + t_{\alpha, \sigma})^\sigma - \tau^\sigma \right) - \left(\sum_{i=1}^L w_{0i} \sum_k \beta_{tki} \right)^2 \\
& \quad + \log p(\sigma) + \log p(\alpha) + \log p(\tau) + \log p(\psi) + \log p(a) + \log p(b), \tag{21}
\end{aligned}$$

where in the last line we have the (independent) priors of the hyperparameters.

6.3 MCMC trace plots for synthetic data

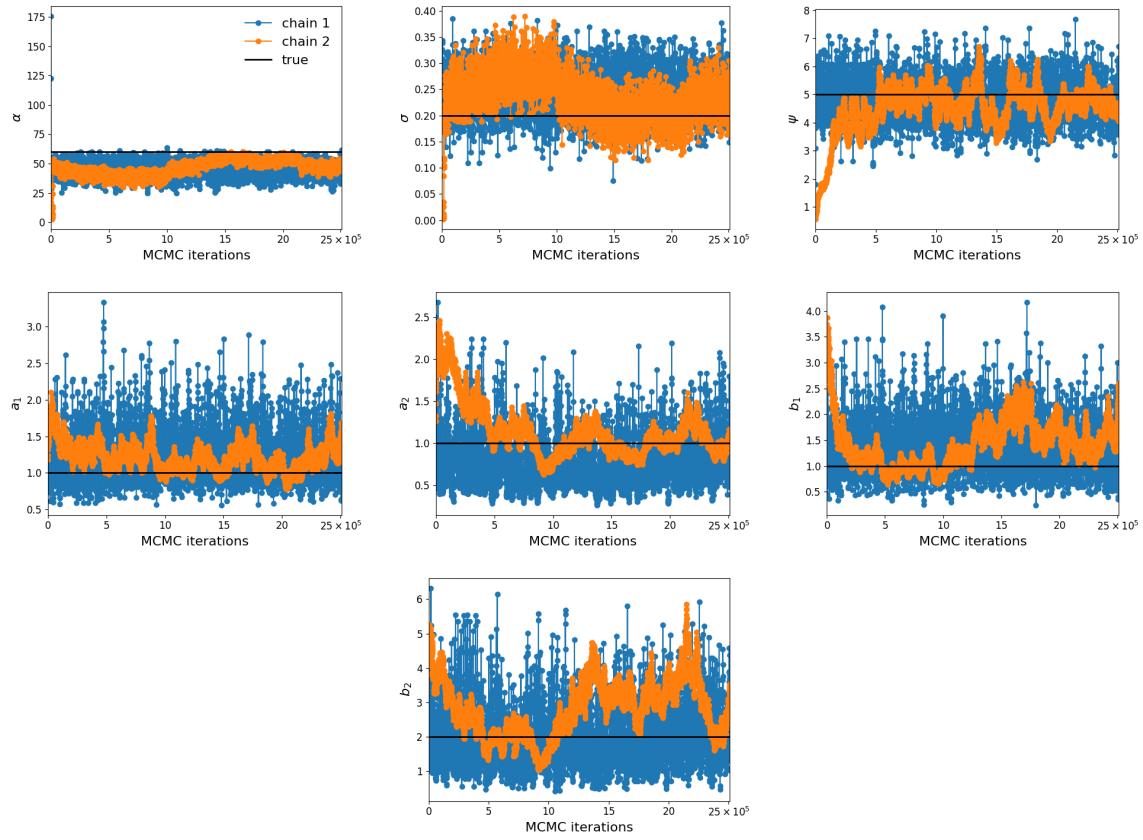


Figure 12: MCMC trace plots for the parameters on the synthetic dataset.

6.4 MCMC trace plots for Reuters news data

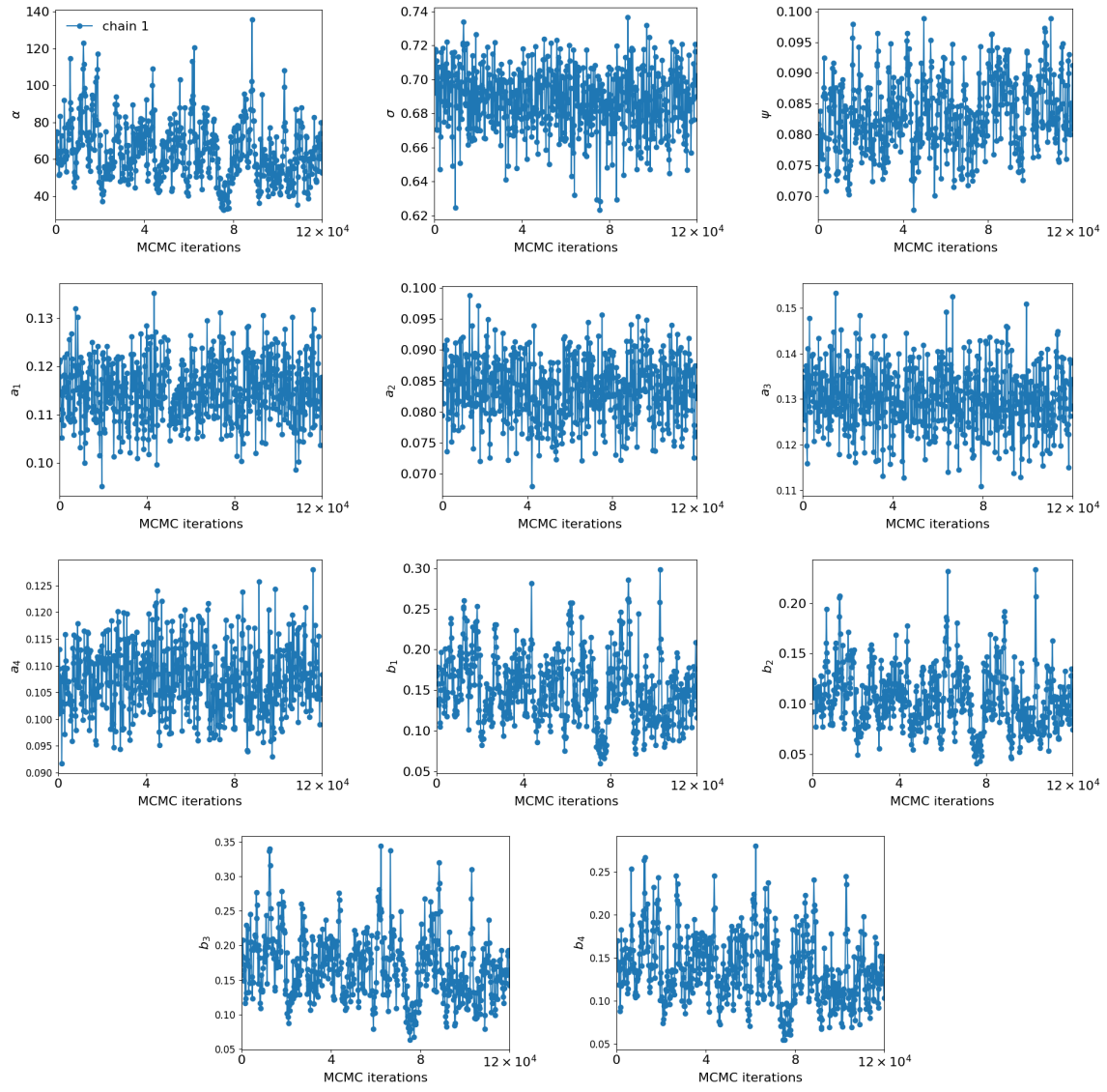


Figure 13: MCMC trace plots of the parameters for the reuters dataset.

6.5 Pie charts of weekly affiliations from SNetOC per time step

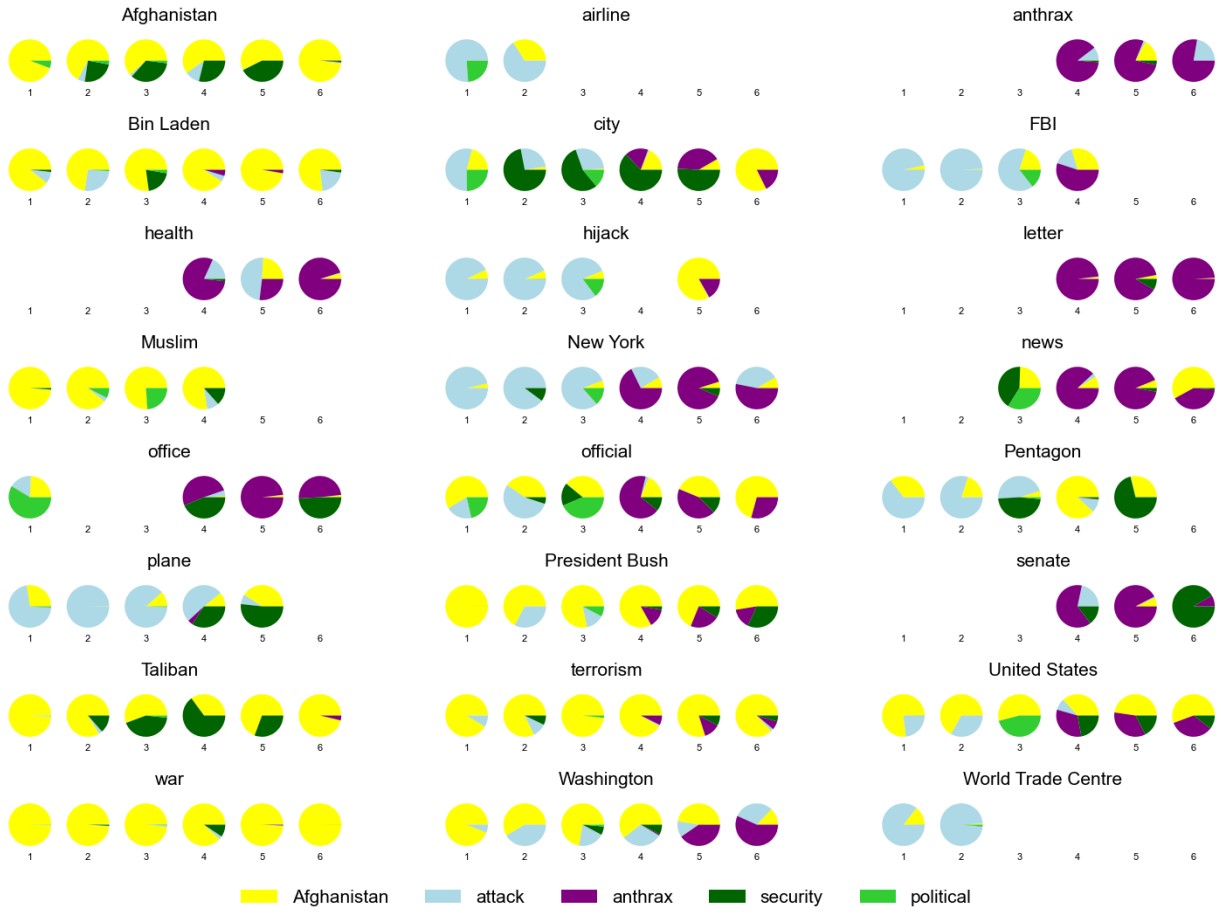


Figure 14: Pie charts with the % of community affiliations for some high degree words at each timestep, using SNetOC at each timestep with $p = 4$.

6.6 Model formulation for dynSBM

Let $\{G_t = (V, E_t)\}_{t=1}^T$ denote a sequence of graphs on a set of N nodes, with symmetric adjacency matrices $Y^{(t)} = [Y_{ij}^{(t)}]_{i,j=1}^N$ (with no self-loops). Each node i is associated with a latent group label $Z_i^{(t)} \in \{1, \dots, p\}$ at time t , which evolves according to a first-order Markov chain: $\Pr(Z_i^{(t)} = q \mid Z_i^{(t-1)} = r) = \Xi_{rq}$, with Ξ the $p \times p$ transition matrix and $\zeta = (\zeta_1, \dots, \zeta_p)$ its initial stationary distribution. Conditional on the latent memberships at time t , edges are independent with $Y_{ij}^{(t)} \mid (Z_i^{(t)} = q, Z_j^{(t)} = \ell) \sim \text{Bernoulli}(\beta_{q\ell}^{(t)})$, where

$\beta_{q\ell}^{(t)} \in [0, 1]$ denote the connection probabilities between groups q and ℓ at time t . Note that the authors also propose ways to treat weighted graphs but none of their approaches includes our Poisson multiedges, hence we need to resort to the binary symmetric graphs.

6.7 Model formulation for dMMSB

Let $\mu^{(t)} = (\mu_1^{(t)}, \dots, \mu_p^{(t)})$ be a mixed membership prior that follows a state-space model $\text{Normal}(\mathbf{A}\mu^{(t-1)}, \Phi)$ initialized at $t = 1$ from $\text{Normal}(\nu, \Phi)$. For each pair of roles r, q an underlying $\eta_{rq}^{(t)}$ compatibility parameter is introduced. At $t = 1$ these are drawn from $\text{Normal}(\iota, \psi)$, and for $t \geq 2$ they follow a state-space model $\eta_{rq}^{(t)} \sim \text{Normal}(\beta\eta_{rq}^{(t-1)}, \psi)$. These are mapped to probabilities via the logistic transform $\beta_{rq}^{(t)} = \exp(\eta_{rq}^{(t)}) / (\exp(\eta_{rq}^{(t)}) + 1)$, yielding a time-indexed role-compatibility matrix $\beta_{rq}^{(t)} \in (0, 1)^{p \times p}$. Edges are generated independently given the latent memberships and compatibilities. For each i, t , the latent group label $Z_i^{(t)} \sim \text{Multinomial}(\pi_i^{(t)}, 1)$, where $\pi_i^{(t)}$ is the mixed membership vector sampled from $\text{LogisticNormal}(\mu^{(t)}, \Sigma^{(t)})$. Conditional on the latent memberships at time t , edges are independent with $Y_{ij}^{(t)} \mid (Z_i^{(t)} = q, Z_j^{(t)} = \ell) \sim \text{Bernoulli}(\beta_{q\ell}^{(t)})$. This construction yields a dynamic mixed-membership network model in which both node-level memberships and role-interaction tendencies evolve over time. The variational EM algorithm described in the paper assumes that the role-compatibility matrix is constant through time and that the transition matrix \mathbf{A} is equal to the identity matrix \mathbf{I} , this reduces the state-space model to a random walk.